Available online at www.sciencedirect.com
ScienceDirect
Tectonophysics 423 (2006) 83–96
TECTONOPHYSICS
www.elsevier.com/locate/tecto

New observational information on the precursory accelerating and decelerating strain energy release

C.B. Papazachos *, G.F. Karakaisis, E.M. Scordilis, B.C. Papazachos

Geophysical Laboratory, University of Thessaloniki, GR54124, Thessaloniki, Greece

Received 4 March 2005; received in revised form 25 October 2005; accepted 25 March 2006
Available online 22 May 2006

Abstract

Recent reliable data are used to study the behavior of seismic activity before 46 strong shallow earthquakes ($M \geq 6.0$), which correspond to five complete samples of mainshocks. These samples include 6 mainshocks ($M=6.0$–7.1) that occurred in western Mediterranean since 1980, 17 mainshocks ($M=6.0$–7.2) which occurred in the Aegean (Greece and surrounding area) since 1980, 5 mainshocks ($M=6.4$–7.5) that occurred in Anatolia since 1980, 12 mainshocks ($M=6.0$–7.3) that occurred in California since 1980 and 6 mainshocks ($M=7.0$–8.3) that occurred in Japan since 1990. In all 46 cases, a similar precursory seismicity pattern is observed. Specifically, it is observed that accelerating Benioff strain (square root of seismic energy) release caused by preshocks occurs in a broad circular region (critical region), with a radius about eight times larger than the fault length of the mainshock, in agreement with results obtained by various research groups during the last two decades. However, in a much smaller circular region (seismogenic region), with a radius about four times the fault length, the corresponding preshock strain decelerates with the time to the mainshock. The time variation of the strain follows in both cases a power law but the exponent power is smaller than unit ($\bar{m}=0.3$) in the case of the accelerating preshock strain and larger than unit ($\bar{m}=3.0$) in the case of the decelerating preshock strain. Predictive properties of this "Decelerating In–Accelerating Out Strain" model are expressed by empirical relations. The possibility of using this model for intermediate-term earthquake prediction is discussed and the relative model uncertainties are estimated.

Keywords: Accelerating strain; Decelerating strain; Earthquake prediction

1. Introduction

Recent investigations indicate that there are two distinct precursory seismicity patterns which have been observed to precede strong earthquakes. The first one concerns accelerating generation of intermediate-magnitude preshocks in a broad region (critical region), while the other corresponds to seismicity quiescence (or decelerating seismicity release) in the narrower region (seismogenic region). Mogi (1969) was the first who proposed a combined form of these patterns, called "doughnut pattern," i.e., quiescence in the seismogenic region of a future mainshock and excitation in the broader surrounding region. A very brief review of both patterns is first attempted.

A large number of observations of the last four decades have shown that many strong ($M \geq 6.5$) earthquakes are preceded by accelerating generation of

* Corresponding author. Tel.: +30 2310998510; fax: +30 2310998528.
E-mail address: costas@lemnos.geo.auth.gr (C.B. Papazachos).

0040-1951/$ - see front matter © 2006 Elsevier B.V. All rights reserved.
doi:10.1016/j.tecto.2006.03.004

intermediate-magnitude preshocks (Tocher, 1959; Raleigh et al., 1982; Papadopoulos, 1986; Sykes and Jaumè, 1990; Knopoff et al., 1996; Tzanis et al., 2000, among others), and that the time variation of the cumulative Benioff strain (square root of seismic energy) follows a power law expressed by the relation:

$$S(t) = A + B(t_c - t)^m \quad (1)$$

where t_c is the origin time of the mainshock, t is the time to the mainshock and A, B, m are parameters which are determined by observations, with $m<1.0$ (Bufe and Varnes, 1993). This behavior of the preshock seismic activity in the broad (critical) region can be physically explained by principles of the critical point dynamics, that is, by considering the process of generation of these moderate-magnitude preshocks as a critical phenomenon, culminating in a large event (mainshock) considered as a critical point (Sornette and Sornette, 1990; Allègre and Le Mouël, 1994; Sornette and Sammis, 1995; Rundle et al., 2000, 2003). The procedure of identifying the critical region has been facilitated by the use of a curvature parameter, C, which was defined by Bowman et al. (1998) as the ratio of the root-mean-square error of the power-law fit (relation (1)) to the corresponding linear fit error, who also showed that the radius, R (in kilometers), of the circular critical region scales with the expected mainshock magnitude, M. Furthermore, Papazachos and Papazachos (2000, 2001) and Papazachos et al. (2005a) have shown that (a) the radius, R (in kilometers), of a circular critical region (or the radius of the circle which has an area equal to the area of the elliptical critical region) scales also negatively with the long-term strain rate, s_a (in Joule$^{1/2}$/year 10^4 km^2) of the critical region; (b) M scales with the mean magnitude, M_{13}, of the three largest preshocks; and (c) the duration, t_a (in years), of the accelerating preshock sequence scales negatively with the strain rate, s_a.

Decrease of seismic energy release in the source region of several strong earthquakes has also been observed by several seismologists during the last three decades. Most of these observations concern the decrease of the number (frequency) of mainly small shocks (seismic quiescence) in the seismogenic region of strong earthquakes (Wyss et al., 1981; Wyss and Habermann, 1988; Scholz, 1988; Chouliaras and Stavrakakis, 2001; Zöller et al., 2002, among others). There are also studies where measures of seismic crustal deformation (Benioff strain, etc.) have been used to show intermediate-term decrease of preshock seismic activity in the seismogenic (fault) region of mainshocks (Kanamori, 1981; Jaumè, 1992; Bufe et al., 1994; Tzanis and Vallianatos, 2003). Simulation models also predict precursory seismic quiescence (Hainzl et al., 2000). This decrease of seismic activity has been attributed to stress relaxation due to preseismic sliding (Wyss et al., 1981; Kato et al., 1997). Papazachos et al. (2004a,b) used data coming mainly from the Aegean area to show that during the critical period, when accelerating seismic strain occurs in the broad critical region, decelerating seismic strain occurs in the narrower seismogenic region. For this reason, the time variation of preshock Benioff strain in the seismogenic region was expressed by a power law (relation (1)) with $m>1$ (a typical value of $m=3.0$). It has been further shown that the length, a (in kilometers), of the seismogenic region, where decelerating seismic strain occurs, scales positively with the mainshock magnitude, M, and negatively with the mean long-term strain rate, s_d (in Joule$^{1/2}$/year 10^4 km^2), and that the duration, t_d, of the decelerating preshock sequence scales negatively with the mean long-term strain rate, s_d. Thus, this "Decelerating In–Accelerating Out Seismic Strain" model seems promising for intermediate-term earthquake prediction.

However, this model has not been extensively tested yet, except for a limited number of earthquakes, and this is the main goal of the present work. In particular, recent reliable data from western Mediterranean, Aegean, Anatolia, California and Japan are used in this study to further test the validity of this model and to improve already proposed or derive new empirical formulas, which relate parameters of the accelerating and decelerating preshock sequences with the mainshock parameters. The importance of these results for intermediate-term earthquake prediction is also discussed.

It should be pointed out that the term "preshocks" used in the present study differs from the classical term "foreshocks," since it corresponds to earthquakes generated in much larger space and time scales. Hence, foreshocks are spatially distributed in the "rupture zone" of an oncoming mainshock and the duration of their sequences is relatively short (of the order of days to months), while preshocks are distributed in a broader region and last much longer (of the order of years). In the present work, we consider two kinds of preshocks, those which are generated in a very broad region (critical region) with an accelerating mode (accelerating preshocks) and those which are generated in the vicinity of the seismogenic zone (fault and neighboring region) with a decelerating mode (decelerating preshocks). It is also shown that all these

preshocks of strong mainshocks ($M \geq 6.0$) are of intermediate magnitude ($M \geq 4.0$).

2. Data

Three samples of data are used for each of the five areas (western Mediterranean, Aegean, Anatolia, California, Japan) considered in the present study. The first sample includes only mainshocks, the second one corresponds to preshocks of each mainshock and the third one uses all shocks to define the long-term mean strain rate release both in each critical region, s_a, and in the seismogenic region which engulfs each fault, s_d. Each sample must be homogeneous (magnitudes in the same scale), large enough (to be representative), accurate (accurate location and magnitude) and complete (including all shocks above a minimum magnitude, M_{min}). In the present work, all magnitudes are moment magnitudes or equivalent to moment magnitudes, that is, magnitudes which have been transformed to moment magnitudes from any other available scale (i.e., M_s, m_b published by ISC and/or NEIC) by using appropriate formulas (Scordilis, 2006). To ensure the relative accuracy of the data, only strong mainshocks ($M \geq 6.0$) that occurred recently (since 1980) were examined. The uncertainties involved are typically less than 30 km for the epicenter and 0.3 for the moment magnitude. A minimum number of 20 preshocks was considered for each preshock sequence to ensure a large enough sample size. The catalogue completeness has been checked by the traditional cumulative frequency–magnitude relation. If we consider the optimum minimum preshock magnitude, M_{min}, for the broader (critical) region for which the best solution (smallest C value) is obtained, the following relation holds:

$$M - M_{min} = 0.54M - 1.91 \quad (2)$$

where M is the mainshock magnitude (Papazachos, 2003; Papazachos et al., 2005a). This relation can be used to estimate the corresponding data threshold which is necessary for investigating accelerating preshock sequences. Thus, for $M = 6.0$, which is the smallest mainshock magnitude considered in the present study, a completeness up to $M_{min} \simeq 4.7$ is necessary for the catalogue to be used. However, the investigation of the decelerating preshock sequences in the seismogenic regions often requires smaller M_{min} values ($M_{min} > 4.0$). For this reason, completeness has been defined for each seismogenic region separately and the value of the minimum preshock magnitude considered for each such region is listed in Table 3. For the calculation of the long-term strain rate for the five examined areas, a minimum magnitude equal to 5.2 was used, similar to our previous work (e.g., Papazachos and Papazachos, 2000, 2001). Such data ($M \geq 5.2$) are complete since 1911 for Mediterranean (W. Mediterranean, Aegean, Anatolia), since 1930 for California and since 1926 for Japan.

For W. Mediterranean (34°N–45°N, 1°W–19°E), all 6 shallow mainshocks with $M \geq 6.0$, for the Aegean (34°N–42°N, 19°E–27°E), all 17 shallow mainshocks with $M \geq 6.0$, and for Anatolia (34°N–42°N, 27°E–40°E), all 5 shallow mainshocks with $M \geq 6.4$, which occurred between 1980 and 2004, were considered. The data for Mediterranean have been taken from a recently compiled catalogue for this area (Papazachos et al., 2005b). Similarly, for California (32°N–42°N, 115°W–125°W) all 12 mainshocks with $M \geq 6.0$ which occurred between 1980 and 2003 were examined. A catalogue has been formed for the purposes of this paper (Karakaisis et al., 2005) which is based on information given by local seismological centers (giving magnitudes in M_L scale), as well as the bulletins of NEIC and ISC (providing magnitudes in M_w, M_s, and m_b scales). Finally, for Japan (30°N–50°N, 130°E–150°E) we have considered the six shallow mainshocks with $M \geq 7.0$ which occurred between 1990 and 2003. The increase of the considered magnitude for Japan was mainly due to its very high seismicity and the large number of $M \geq 6.4$ closely distributed in both time and space, which made the application of the proposed method almost impossible. A catalogue for Japan has also been created (Scordilis et al., 2005) which is based on data published by the Japanese Meteorological Agency (JMA), as well as by NEIC and ISC. Thus, for 46 shallow strong ($M = 6.0–8.3$) earthquakes, which form five complete samples of mainshocks and which have occurred in five different seismotectonic regimes, recent reliable data were available for the study of the observational properties of the critical region and of the seismogenic region. The dates, epicenter coordinates, $E(\varphi,\lambda)$, and moment magnitudes, M, for these 46 mainshocks are listed in Table 1. The epicenters of these mainshocks are shown in Fig. 1.

It must be emphasized that strong preshocks, strong aftershocks, strong off-fault aftershocks (which occur shortly after the mainshock at some distance) and strong late aftershocks (which occur after some years in the fault region of the mainshock) have critical regions and critical periods which partially coincide with the critical region and period of their mainshock. Thus, the critical regions and periods of these

Table 1
The origin time, t_c, epicenter geographic coordinates, $E(\varphi,\lambda)$, moment magnitude, M, center of region of decelerating strain, $F(\varphi,\lambda)$, center of region of accelerating strain, $Q(\varphi,\lambda)$, and retrospectively predicted epicenter, $E^*(\varphi,\lambda)$, origin time, t_c^*, and magnitude, M^*, for each of the 46 mainshocks examined in this study

Area	t_c	$E(\varphi,\lambda)$	M	$F(\varphi,\lambda)$	$Q(\varphi,\lambda)$	$E^*(\varphi,\lambda)$	t_c^*	M^*
W. Mediterranean								
1	1980.10.10	36.2, 01.4	7.1	35.7, 02.4	36.2, 00.6	36.4, 00.8	1981.5	6.8
2	1980.11.23	40.8, 15.3	6.9	42.0, 14.3	44.0, 13.8	41.1, 13.9	1980.8	6.7
3	1996.09.05	42.5, 18.0	6.0	43.7, 18.8	42.8, 14.9	43.3, 17.7	1997.2	6.1
4	1997.09.26	43.0, 12.9	6.0	44.2, 12.1	44.0, 14.9	44.1, 13.0	1997.6	5.9
5	2002.09.06	41.0, 15.0	6.0	41.9, 14.6	43.0, 16.0	41.9, 14.6	2002.0	6.4
6	2003.05.21	36.9, 03.8	6.8	35.7, 05.0	38.6, 06.0	36.8, 05.4	2003.4	7.0
Aegean								
1	1980.07.09	39.3, 22.9	6.5	39.6, 21.9	37.8, 24.1	38.9, 22.5	1981.8	6.2
2	1981.02.24	38.1, 23.0	6.7	38.1, 24.0	36.8, 21.7	37.9, 23.1	1980.1	7.0
3	1981.12.19	39.0, 25.3	7.2	38.0, 24.3	37.0, 23.1	38.3, 24.1	1980.2	7.2
4	1983.01.17	38.1, 20.2	7.0	38.5, 19.5	37.4, 18.7	38.5, 19.9	1983.2	6.7
5	1984.06.21	35.4, 23.3	6.2	35.4, 25.0	35.9, 25.5	35.2, 25.0	1986.0	6.0
6	1986.09.13	37.1, 22.1	6.0	35.9, 22.3	36.4, 21.1	35.9, 22.2	1986.1	5.8
7	1990.06.16	39.1, 20.7	6.0	39.1, 19.5	40.6, 20.9	39.2, 19.7	1991.6	6.0
8	1992.04.30	35.1, 26.6	6.1	35.9, 25.8	35.6, 27.6	35.8, 25.9	1992.7	6.0
9	1992.11.06	38.1, 27.0	6.2	39.1, 26.0	37.1, 27.5	38.3, 26.7	1994.0	6.3
10	1995.05.13	40.2, 21.7	6.6	39.3, 21.4	41.2, 21.4	39.2, 21.2	1995.0	6.7
11	1996.07.20	36.1, 27.5	6.2	35.1, 28.0	34.6, 28.3	35.3, 27.7	1999.5	6.3
12	1997.10.13	36.4, 22.2	6.4	36.4, 23.0	37.0, 22.2	36.3, 22.9	1995.4	6.4
13	1997.11.18	37.5, 20.7	6.6	37.0, 21.6	39.6, 21.8	38.1, 21.1	1996.7	6.9
14	1999.09.07	38.1, 23.5	6.0	38.3, 24.0	37.1, 25.7	37.9, 24.7	2000.0	6.4
15	2001.07.26	39.1, 24.4	6.4	38.3, 24.1	37.6, 26.4	38.2, 25.0	2000.4	6.6
16	2003.08.14	38.7, 20.5	6.3	38.7, 21.0	37.7, 19.0	38.7, 20.7	2004.0	6.4
17	2004.03.17	34.6, 23.3	6.0	34.6, 22.1	34.6, 24.6	34.7, 23.2	2001.5	6.3
Anatolia								
1	1983.07.05	40.2, 27.3	6.4	40.2, 28.1	38.2, 26.0	39.3, 27.5	1982.6	6.5
2	1992.03.13	39.7, 39.6	6.6	38.7, 39.1	37.7, 38.9	39.5, 39.5	1993.5	6.3
3	1995.10.01	38.1, 30.2	6.4	39.1, 30.2	35.7, 28.2	38.3, 29.5	1996.8	6.5
4	1996.10.09	34.5, 32.1	6.8	35.0, 31.4	34.3, 30.3	35.2, 31.4	1997.6	6.4
5	1999.08.17	40.8, 30.0	7.5	40.6, 31.5	38.6, 29.5	39.7, 30.1	1999.6	7.3
California								
1	1980.05.25	37.6, −118.8	6.2	38.1,−119.3	37.6,−116.6	37.9,−118.2	1978.9	6.3
2	1980.11.04	41.1, −124.6	7.3	42.1,−124.1	41.6,−125.6	42.0,−124.5	1981.0	7.0
3	1983.05.02	36.2, −120.3	6.4	35.0,−120.3	38.0,−122.5	35.9,−120.8	1983.3	6.2
4	1984.04.24	37.3, −121.7	6.2	37.0,−123.1	38.1,−122.5	38.0,−122.3	1984.5	6.3
5	1987.11.24	33.0, −115.9	6.6	32.0,−116.9	35.4,−118.3	33.2,−117.0	1987.8	6.9
6	1989.10.18	37.1, −121.9	6.9	36.3,−123.1	37.6,−122.4	37.1,−121.7	1989.6	7.0
7	1992.04.25	40.3, −124.2	7.1	39.3,−123.2	37.3,−123.2	39.6,−123.5	1987.7	7.1
8	1992.06.28	34.2, −116.4	7.3	35.8,−116.4	33.5,−116.9	35.1,−116.9	1992.6	7.1
9	1993.05.17	37.2, −117.8	6.1	36.5,−116.8	35.0,−116.6	36.8,−117.1	1993.6	6.1
10	1993.09.21	42.3, −122.0	6.0	41.1,−123.0	40.8,−123.0	41.6,−122.1	1994.2	6.3
11	1994.01.17	34.2, −118.5	6.6	33.2,−119.5	34.9,−119.0	33.5,−119.3	1995.1	6.8
12	2003.12.22	35.7, −121.1	6.5	35.7,−122.1	33.7,−120.9	35.5,−121.2	2004.3	6.6
Japan								
1	1993.07.12	42.9, 139.2	7.7	41.5, 139.7	45.3, 136.8	42.3, 139.7	1993.6	7.5
2	1994.10.04	43.7, 147.4	8.3	43.1, 146.6	41.7, 148.4	43.3, 147.2	1994.9	8.1
3	1995.01.16	34.6, 135.0	7.0	35.3, 135.0	35.4, 133.2	35.1, 135.4	1995.5	6.8
4	2003.05.26	38.8, 141.6	7.0	39.5, 141.8	38.1, 139.6	39.0, 142.7	2003.8	7.0
5	2003.09.25	41.8, 143.9	8.3	42.3, 143.4	41.8, 143.4	42.1, 143.4	2003.8	8.4
6	2003.10.31	37.8, 142.6	7.0	37.1, 143.6	39.8, 141.1	38.0, 142.7	2004.9	7.0

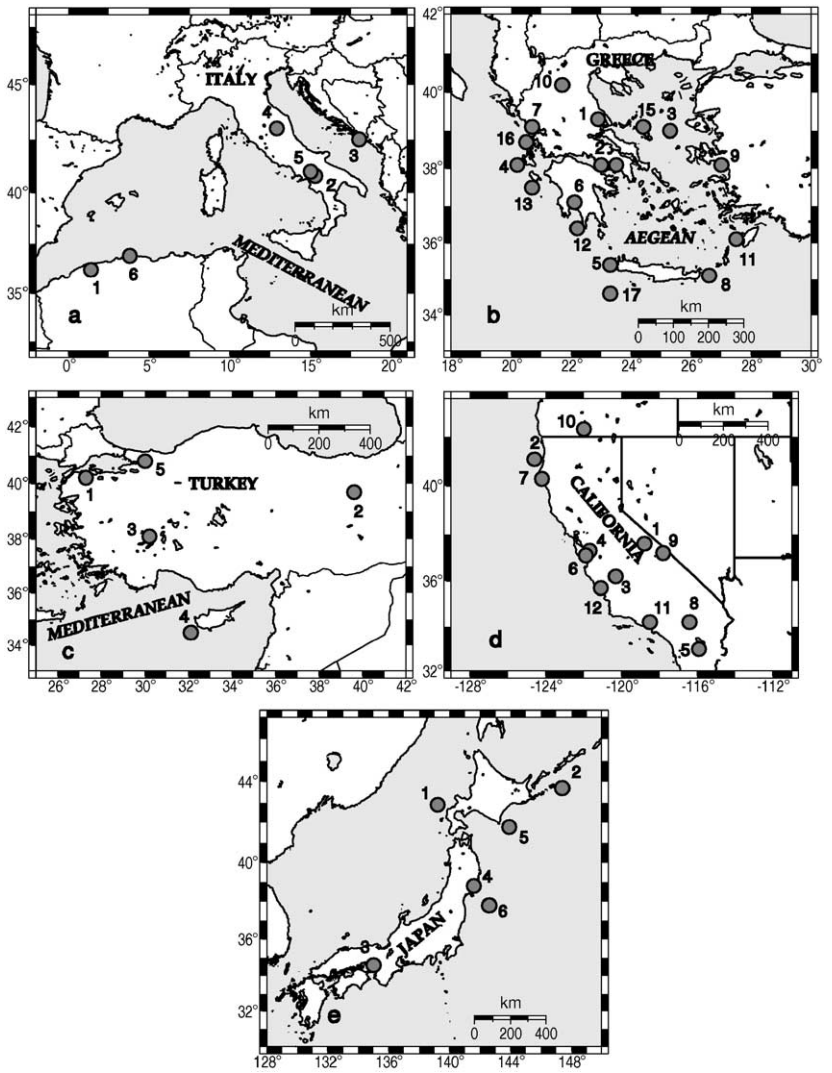

Fig. 1. Epicenters of the 6 mainshocks in western Mediterranean (a), 17 mainshocks in the Aegean (b), 5 mainshocks in Anatolia (c), 12 mainshocks in California (d) and 6 mainshocks in Japan (e), of which accelerating and decelerating preshock sequences are investigated in the present work. The numbers close to the epicenters correspond to the code numbers in Tables 1–3.

associated shocks cannot be distinguished, and for this reason, no analysis for such shocks has been performed in the present work.

3. Procedure followed

In order to identify the critical region of an already occurred mainshock, an algorithm developed by Papazachos (2001) has been used. According to this algorithm, the broad seismic zone (e.g., of dimensions 300 km × 300 km) where the mainshock is located is separated in a grid of points with the desired density (e.g., 0.2°NS, 0.2°EW). Each grid point is considered as the center of the circular critical region and data of earthquakes (preshocks) which are located in this region are used to calculate the cumulative Benioff strain and estimate through optimization parameters A and B of relation (1), as well as the curvature parameter, C. For this estimation, the origin time of the known mainshock (parameter t_c) was considered as constant and the minimum magnitude, M_{min}, of preshocks was estimated by relation (2) from the magnitude, M, of the mainshock. The exponent of relation (1), m, was taken equal to the mean value (=0.3) determined or adopted in similar studies (e.g., Zöller and Hainzl, 2002), in agreement with theoretical considerations and laboratory results (Ben-Zion et al., 1999; Guarino et al., 1999; Rundle et al., 2000; Ben-Zion and Lyakhovsky, 2002),

Table 2
Parameters of the 46 critical regions

Area	R	logs_a	t_{sa}	M_{min}	n	C	P	q_a
W. Mediterranean								
1	277	4.88	1912	5.1	21	0.50	0.55	3.7
2	338	5.36	1945	5.2	53	0.50	0.98	6.5
3	183	5.39	1963	4.8	40	0.38	0.83	7.2
4	160	5.15	1953	4.8	24	0.57	0.75	4.4
5	198	5.35	1963	4.7	54	0.47	0.97	6.8
6	770	4.58	1924	5.2	96	0.50	0.56	3.7
Aegean								
1	137	5.52	1954	4.6	37	0.47	0.81	5.8
2	268	5.92	1967	5.1	45	0.50	0.64	4.3
3	277	5.94	1967	5.1	47	0.58	0.74	4.2
4	237	5.77	1963	4.9	32	0.50	0.86	5.7
5	115	5.62	1960	4.6	27	0.48	0.79	5.5
6	104	5.78	1965	4.6	27	0.44	0.72	5.4
7	184	5.80	1971	4.7	75	0.28	0.62	7.4
8	185	5.91	1976	4.8	70	0.28	0.57	6.8
9	129	5.90	1976	4.8	43	0.43	0.75	5.8
10	168	5.71	1973	5.0	21	0.41	0.87	7.1
11	230	5.69	1974	4.8	100	0.20	0.59	9.6
12	138	5.93	1970	4.8	81	0.40	0.67	5.5
13	181	6.12	1985	5.0	27	0.39	0.69	5.9
14	164	5.63	1975	4.7	43	0.44	0.80	6.1
15	163	5.74	1980	5.0	34	0.44	0.81	6.1
16	137	5.56	1984	4.7	29	0.46	0.55	4.0
17	136	5.72	1982	4.8	49	0.40	0.92	7.6
Anatolia								
1	142	5.70	1960	4.7	21	0.52	0.82	5.2
2	175	4.76	1912	5.0	21	0.36	0.62	5.8
3	226	5.83	1977	4.8	108	0.28	0.66	7.8
4	200	4.89	1930	4.8	34	0.46	0.62	4.5
5	310	5.79	1980	5.1	35	0.45	0.69	5.1
California								
1	222	5.31	1942	5.0	46	0.56	0.71	4.2
2	249	5.65	1957	5.1	29	0.51	0.49	3.2
3	218	5.09	1931	4.7	65	0.41	0.81	6.5
4	175	5.19	1939	4.8	33	0.39	0.60	5.1
5	283	5.57	1961	5.0	83	0.48	0.81	5.6
6	375	5.16	1943	5.2	93	0.43	0.89	7.0
7	431	5.20	1943	5.1	139	0.48	0.80	5.6
8	468	5.28	1953	5.2	86	0.39	0.66	5.6
9	149	5.45	1962	4.7	22	0.41	0.62	5.0
10	132	5.33	1957	4.7	22	0.53	0.63	3.9
11	186	5.66	1972	4.8	21	0.36	0.81	7.5
12	375	5.15	1956	4.9	76	0.48	0.59	4.1
Japan								
1	636	5.32	1955	5.6	46	0.55	0.63	3.8
2	782	6.10	1982	5.6	158	0.49	0.87	5.9
3	693	5.69	1972	5.1	285	0.36	0.48	4.4
4	201	6.01	1989	4.9	70	0.48	0.60	4.2
5	1340	5.79	1984	5.8	273	0.76	0.88	3.9
6	180	6.28	1997	5.0	32	0.29	0.58	6.7

which suggest exponent values between 0.25 and 0.33. Calculations for each point of the grid are repeated for a large set of values of the radius, R (in kilometers), of the circular region and of the starting time, t_{sa} (in years), of the sequence. The geographic point, $Q(\varphi,\lambda)$, with the smallest C value, was considered as the center of the critical region and the solution, (C,R,t_{sa}), for this point was adopted as the best solution. The geographic coordinates of the center, $Q(\varphi,\lambda)$, of all 46 critical regions are listed in Table 1, while the values of the parameters C, R, t_{sa}, logs_a, of the best solutions are given in Table 2.

For the seismogenic region of each of the 46 mainshocks, circular shapes were also assumed. In order to study the decelerating behavior of each source region, the area around the fault (with dimensions, e.g., 150 km × 150 km or larger depending on the mainshock magnitude) was also separated in a grid of points with the desired density (e.g., 0.1°NS, 0.1°EW) and each point of the grid was considered as center of the circular region. A similar procedure was used in order to calculate parameters A and B of relation (1) and the curvature parameter, C, keeping constant the origin time, t_c, and the mainshock magnitude, M. The exponent parameter m was allowed to vary and values distributed around a mean value equal to 3.0 were found. Although no theoretical results exist yet to support the choice of this value for the decelerating deformation exponent, we have decided to keep this value fixed in order to avoid fluctuations due to data errors, similarly to what was previously mentioned for the accelerating deformation exponent. Calculations for each geographic point were repeated for a large number of lengths of the circle radius a (in kilometers), and the starting time, t_{sd} (in years), of the seismic sequence. Calculations were also repeated for several minimum magnitudes, M_{min}, of decelerating preshocks in order to define the value of this magnitude which corresponds to the best solution (smallest C value) and correlate it with the mainshock magnitude (relation (12)). The geographic point, $F(\varphi,\lambda)$, with the smallest C value, was considered as the center of seismogenic region and the solution (C,a,t_{sd}) for this point was adopted as the best solution. The

Notes to Table 2:
The numbers in the first column correspond to the code numbers of the Table 1, R (in km) is the radius of the circular critical region, s_a(in Joule$^{1/2}$/year 10^4 km^2) is the strain rate in the critical region, t_{sa} is the start year of the accelerating preshock sequence, M_{min} is the magnitude of the smallest preshock, n is the number of preshocks, C is the curvature parameter, P is the probability that the particular preshock sequence fit the global relations (3,4,5), and q_a is the quality index defined by relation (6).

Table 3
Parameters of the decelerating preshock sequences, which occurred in the 46 seismogenic regions

Area	a	$\log s_d$	t_{sd}	M_{min}	n	C	P	q_d
W. Mediterranean								
1	272	4.28	1955	4.3	84	0.28	0.50	5.4
2	178	5.25	1960	4.3	142	0.51	0.99	5.9
3	110	5.24	1976	4.1	65	0.41	0.96	7.0
4	109	5.27	1970	4.1	66	0.19	0.54	8.6
5	113	5.23	1980	4.0	66	0.42	0.85	6.0
6	220	4.29	1961	4.4	46	0.39	0.92	7.0
Aegean								
1	98	6.02	1969	4.2	61	0.26	0.72	8.4
2	133	5.94	1964	4.4	126	0.28	0.51	5.4
3	172	5.87	1964	4.5	156	0.27	0.56	6.1
4	105	5.88	1970	4.5	103	0.22	0.55	7.4
5	99	5.70	1972	4.2	66	0.30	0.55	5.5
6	62	5.69	1972	4.1	59	0.28	0.48	5.2
7	91	5.93	1980	4.1	40	0.28	0.62	6.6
8	99	5.72	1978	4.2	79	0.48	0.91	5.7
9	103	5.88	1982	4.2	115	0.35	0.63	5.3
10	138	5.80	1981	4.4	236	0.29	0.81	8.3
11	110	5.67	1987	4.3	59	0.33	0.47	4.3
12	117	5.84	1984	4.3	58	0.44	0.91	6.3
13	140	5.71	1981	4.3	570	0.48	0.66	4.1
14	88	5.87	1987	4.1	37	0.35	0.87	7.6
15	113	5.94	1987	4.2	80	0.35	0.68	5.9
16	95	6.00	1992	4.2	167	0.34	0.81	7.3
17	111	5.37	1980	4.2	111	0.38	0.55	4.3
Anatolia								
1	119	5.72	1968	4.3	92	0.45	0.88	5.9
2	122	5.46	1975	4.2	26	0.25	0.73	8.8
3	131	5.72	1983	4.2	45	0.28	0.56	5.9
4	164	5.34	1977	4.3	24	0.44	0.97	6.6
5	230	5.50	1982	4.5	31	0.43	0.95	6.6
California								
1	115	5.50	1960	4.2	43	0.18	0.69	11.3
2	136	5.25	1960	4.4	22	0.37	0.52	4.2
3	103	5.34	1964	4.1	22	0.32	0.62	5.8
4	133	4.97	1959	4.2	28	0.33	0.93	8.5
5	159	5.20	1966	4.3	37	0.47	0.93	6.0
6	166	5.18	1967	4.4	25	0.38	0.77	6.2
7	201	5.26	1967	4.4	117	0.34	0.63	5.6
8	246	5.11	1969	4.6	108	0.38	0.86	6.8
9	108	5.49	1969	4.1	120	0.29	0.55	5.7
10	120	5.38	1975	4.1	28	0.50	0.78	4.7
11	144	5.33	1975	4.1	21	0.52	0.88	5.1
12	141	5.14	1982	4.3	24	0.37	0.84	6.8
Japan								
1	203	6.21	1984	4.5	200	0.21	0.82	11.6
2	291	6.04	1975	4.8	1629	0.28	0.50	5.3
3	142	5.86	1983	4.5	108	0.27	0.67	7.4
4	126	6.55	1996	4.3	360	0.45	0.81	5.3
5	199	6.29	1994	4.8	159	0.27	0.61	6.8
6	127	6.42	1994	4.3	157	0.31	0.76	7.4

geographic coordinates of the centers, $F(\varphi,\lambda)$, of the 46 seismogenic regions are listed in Table 1 and the values of the parameters C, a, t_{sd}, $\log s_d$, of the best solutions are given in Table 3.

Fig. 2 presents graphically an indicative example for each of the five investigated areas, which shows the circular critical (accelerating deformation) region, the circular (decelerating deformation) seismogenic region and the corresponding time variation of the accelerating and decelerating strain.

4. Accelerating seismic strain in the critical region

It has been recently shown (Papazachos et al., 2005a) that the logarithm of the radius, R (in kilometers), of a circular critical region (or the radius of the circle with area equal to the area of an elliptical critical region) scales with the mainshock magnitude, M, and with the long-term strain rate, s_a (in Joule$^{1/2}$/year 10^4 km^2), according to the relation

$$\log R = 0.42M - 0.30\log s_a + 1.25, \quad \sigma = 0.15 \qquad (3)$$

where σ is the standard deviation. This relation is in excellent agreement with the theoretical results derived by Dobrovolsky et al. (1979), who adopted a model of an elastic soft inclusion in a more rigid elastic space in order to determine the region of precursory deformation for a future earthquake. Data from the 46 mainshocks examined in the present study also fit well with relation (3). In general, the radius of the critical region is about eight times larger than the fault length of the corresponding mainshock, similar to what has been found in earlier studies (Bowman et al., 1998).

Also, Papazachos (2003) and Papazachos et al. (2005a) have proposed the following relation:

$$M = M_{13} + 0.60, \quad \sigma = 0.20 \qquad (4)$$

between the mainshock magnitude, M, and the mean magnitude, M_{13}, of the three largest accelerating preshocks, which is also well fitted by the data of the present work.

Notes to Table 3:
The numbers in the first column correspond to the code numbers of Table 1. a (in km) is the length of the radius of the seismogenic region, s_d (in Joule$^{1/2}$/year 10^4 km^2) is the strain rate in the seismogenic region, t_{sd} is the start year of the decelerating preshock sequence, M_{min} is the magnitude of the smallest preshock, n is the number of preshocks, C is the curvature parameter, P is the probability that the particular preshock sequence fit the global relations (8) and (9) and q_d is the quality index defined by relation (10).

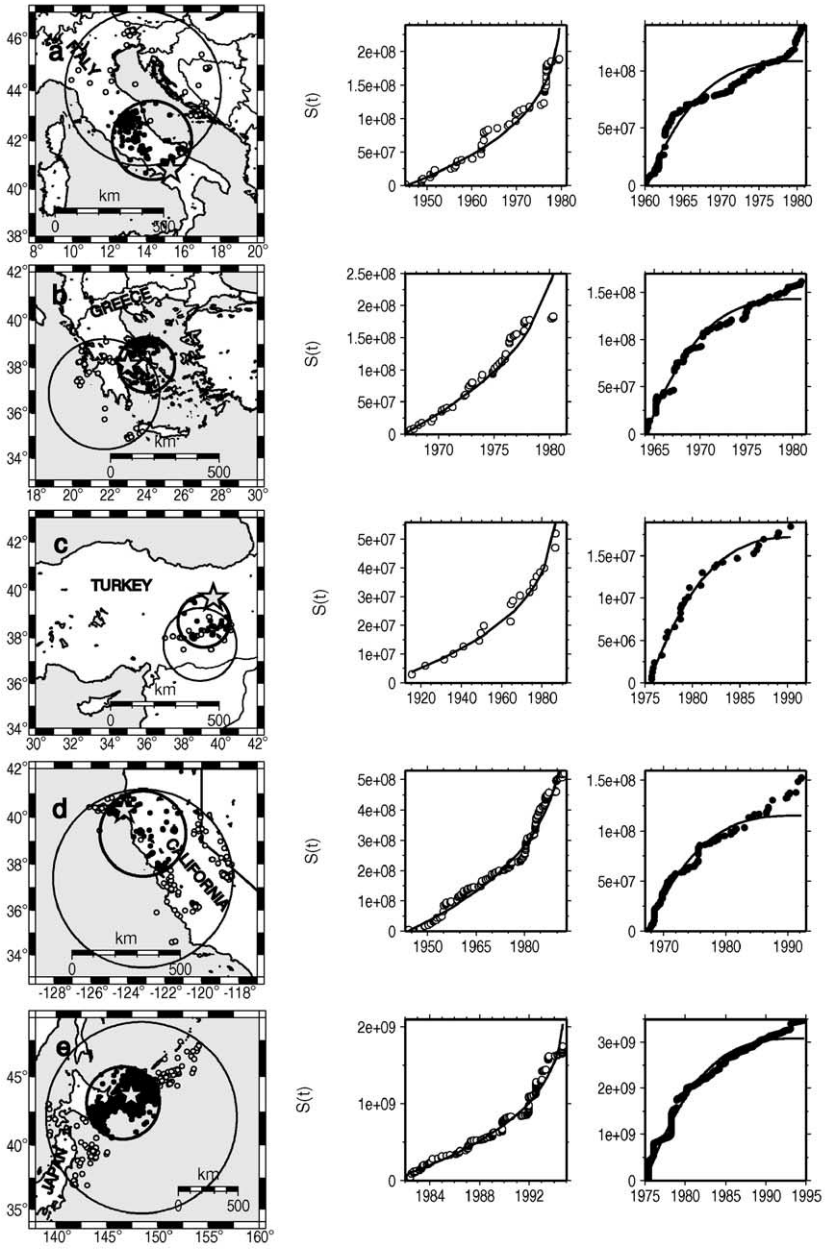

Fig. 2. Five examples of accelerating–decelerating seismic sequences for the mainshocks of (a) 23 November 1980 in W. Mediterranean, (b) 24 February 1981 in Greece, (c) 13 March 1992 in Anatolia, (d) of 25 April 1992 in central California, and (e) 4 October 1994 in Japan. Epicenters of mainshocks are indicated by stars, of accelerating preshocks in the circular critical regions by open circles and of decelerating preshocks in the circular (seismogenic) regions by solid circles. On the right of each map, the time variation of the cumulative Benioff strain, $S(t)$, is given for the accelerating sequence (left plot) and decelerating sequence (right plot). Solid lines represent fitting to the data of a power law (relation (1)).

Values of t_c, t_{sa} and s_a, listed in Tables 1 and 2, for critical regions are used to derive a relation between the duration of a preshock sequence and s_a. Fig. 3 shows the variation of the logarithm of the total duration, $t_a = t_c - t_{sa}$ (in years), of the accelerating preshock sequence as a function of $\log s_a$. The data are fitted by the following relation, in the least squares' sense:

$$\log(t_c - t_{sa}) = 4.60 - 0.57 \log s_a, \quad \sigma = 0.10 \tag{5}$$

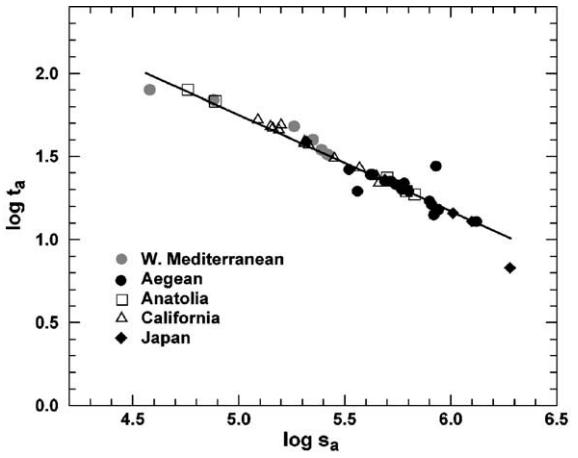

Fig. 3. Plot of the logarithm of the duration, t_a, (in years), of the accelerating preshock sequences as a function of the logarithm of the long-term strain rate, s_a (in Joule$^{1/2}$/year 10^4 km^2).

which can be used to calculate the origin time, t_c, of an ensuing mainshock, if the start of the accelerated deformation period can be defined.

In addition to the fit of the time variation of the Benioff strain by a power-law (relation (1)), relations (3)–(5) can be considered as additional constraints to the pattern of accelerating strain and the critical earthquake model. To quantify it, Papazachos and Papazachos (2001) have calculated the conditional probability for the three parameters (R,M,t_a) in these relations, assuming that the deviation of each parameter with respect to its expected value follows a Gaussian distribution. The average, P, of these probabilities was used as a measure of the agreement of the determined parameters for a particular sequence with these three global relations. Using this probability, a "quality index", q_a, has been defined (Papazachos et al., 2002) for each point of the investigated area using the equation

$$q_a = \frac{P}{m*C} \tag{6}$$

This index, q_a, is of importance for identifying centers of critical regions of expected mainshocks, since its value increases with increasing probability, P, indicating that the examined point fulfills the global relations (3)–(5) and with increasing deviation from linearity (small values of curvature parameter C). The m value is considered constant (m=0.3) in this work, but we keep it in this formula because it can have a different value in some cases. Values of P and q_a for the center of the 46 critical regions investigated in the present work are also listed in Table 2. Examination of these values from Table 1 shows that the following cut-off values can be derived:

$$C \leq 0.60, \quad P \geq 0.45, \quad q_a \geq 3.0 \tag{7}$$

since all events in Table 1 fulfill the above criteria, except a single case where C exhibits a larger value (=0.76).

5. Decelerating seismic strain in the seismogenic region

From the data presented in Tables 1 and 3, the following relation can be derived between the length, a (in kilometers), of the radius of the circular seismogenic region, the magnitude, M, of the corresponding mainshock and the strain rate, s_d (in Joule$^{1/2}$/year 10^4 km^2):

$$\log a = 0.23M - 0.14 \log s_d + 1.40, \quad \sigma = 0.10 \tag{8}$$

Fig. 4 shows a plot of the logarithm of the duration, $t_d = t_c - t_{sd}$, of each decelerating preshock sequence as a function of the logarithm of the long-term mean strain rate, s_d in (Joule$^{1/2}$/year 10^4 km^2), leading to the relation

$$\log(t_c - t_{sd}) = 2.95 - 0.31 \log s_d, \quad \sigma = 0.12 \tag{9}$$

This relation, which is similar to Eq. (5), can be also used in a similar manner to estimate the origin time, t_c, of an ensuing mainshock in a seismogenic region, once the initiation time of the decelerating deformation period is defined.

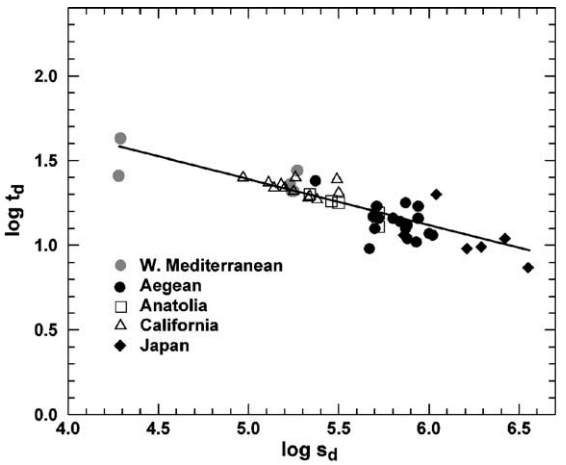

Fig. 4. The logarithm of the duration, t_d (in years), of the decelerating preshock sequences as a function of the logarithm of the long-term strain rate, s_d (in Joule$^{1/2}$/year 10^4 km^2).

A quality index, q_d, can be also defined by the relation

$$q_d = \frac{P^* m}{C} \quad (10)$$

where P is the probability that preshock observations in a seismogenic region are compatible with relations (8) and (9). Similar to relation (7), the values of C, P and q_d, listed in Table 3 for the seismogenic regions can be used to derive the following cut-off values with which all examined earthquakes comply

$$C \leq 0.60, \quad P \geq 0.45, \quad q_d \geq 3.0 \quad (11)$$

when using an exponent value $m=3.0$.

Application of least squares on the values of M and M_{min} listed in Tables 1 and 3 gives

$$M - M_{min} = 0.71M - 2.35, \quad \sigma = 0.10 \quad (12)$$

which gives the smallest magnitude of a decelerating preshock sequence for which a best solution is obtained. Thus, for mainshock magnitudes 6.0, 7.0 and 8.0, the corresponding values of M_{min} are 4.1, 4.4 and 4.7, respectively. That is, decelerating preshock seismicity pattern is also prominent mainly for intermediate-magnitude preshocks.

6. Tests on random catalogues

The results previously presented concern the a posteriori analysis of past events in order to define the main characteristics of the proposed seismicity pattern. However, it is clear that such retrospective analysis is not enough for a complete evaluation of the uncertainties involved in the proposed pattern, especially if we would like to apply it for earthquake prediction. For this reason, the results obtained in the present study were also checked for the possibility that the identified "Decelerating In–Accelerating Out Strain" seismic deformation pattern could also have occurred even from a random data distribution. Such tests have been traditionally used in similar studies (e.g., Bowman et al., 1998; Zöller et al., 2001) by applying the proposed detection method on synthetic random catalogues. Using this approach, we can assess the probability that the obtained results correspond to a real observational pattern or that the identified patterns could be due to the data randomness and the large parametric space examined for the critical area (e.g., ellipticity, azimuth, size, duration of preshock period, etc.).

As a test area from the five studied areas, we have chosen the Aegean area for which detailed information for its seismotectonic setting and seismicity parameters were available from earlier studies. Furthermore, the Aegean is among the highest seismicity areas (large annual deformation rates; see Figs. 3 and 4); hence, the synthetic catalogues will contain a very large number of events, allowing the full exploration of artifacts that can arise in a large catalogue due to the multiple parameter optimization used in the present work. For the generation of the synthetic but also "realistic" random catalogues, we have adopted a modified version of the approach proposed by Zöller et al. (2001). Specifically,

(a) The original earthquake catalogue for the Aegean was initially declustered from its aftershocks. For the aftershock sequence duration, we used the results of Papazachos (1974a,b) and Papazachos and Papazachou (1997), while for the aftershock area, we used a circular region with a radius, R, given by

$$\log R = 0.19M + 0.36 \quad (13)$$

which was defined by the use of all aftershock sequences in Greece and surrounding area.

(b) On the basis of the declustered catalogue and the application of Poisson time distribution for the occurrence times and the Gutenberg–Richter relation for the magnitude distribution of each seismogenic zone defined for the Aegean area using the zonation of Papaioannou and Papazachos (2000), we estimated the corresponding random epicenter distributions in space and time. In this way, the seismicity distribution of the random catalogue is adapted (equivalent) to the declustered catalogue.

(c) Aftershocks following the time pattern proposed by Mogi (1962) and adapted by Papazachos (1974b) for the Aegean area, as well as Eq. (13) for their spatial distribution were added to the random catalogues to calculate the final synthetic catalogues, in order to include the "realistic" pattern of aftershock sequences.

In order to test the efficiency of the proposed algorithm, a large number of random catalogues has been created. From each catalogue, a random set of mainshocks were selected and the same processing was performed for all mainshocks, as if they corresponded to real earthquakes. In all cases, results for deceleration and acceleration were obtained for those cases that fulfilled Eqs. (7) and (11), similar to the behavior of the 46 events studied in the present work.

The results obtained were surprisingly different for the accelerating and the decelerating patterns. For the acceleration of the broader critical region, in many cases, it was possible to identify a false acceleration

pattern that could be associated (distances up to ~250 km) with the examined mainshocks. The final cumulative distribution of the obtained q_a values from random catalogues is presented against the corresponding distribution from Table 2 in Fig. 5. It is important to note that for almost the entire range of q_a values, the observed distribution exhibits much higher probability values than the corresponding distribution from random catalogues. For instance, the minimum q_a value observed from data of the Aegean area (=4.0), has a probability less than 70% to be randomly observed, as tests with random data indicate.

It should be pointed out that the obtained probabilities from random catalogues are still quite high, given the fact that additional constrains (Eqs. (3)–(5) and (7)) are used when searching for the accelerated deformation pattern. Therefore, observation only of the accelerated deformation pattern has a high probability to occur randomly, e.g., a q_a value of 6 corresponds to a 30% probability of random occurrence. However, this problem has a marginal effect on the results obtained in the present work due to the fact that in only 10% of the examined cases could a decelerating deformation pattern be observed when random catalogues were used, with q_d values smaller than 4.5. Therefore, the probability of the simultaneous occurrence of accelerating and decelerating deformation patterns associated with a mainshock due to the catalogue randomness is about one order of magnitude less than the one observed from Fig. 5.

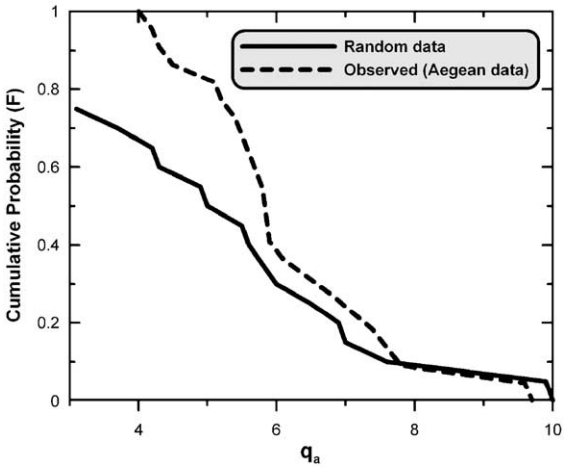

Fig. 5. Comparison of the cumulative probability density of the q_a values for the observed Aegean data (dashed line) and the corresponding distribution from artificial random catalogues (solid line). Notice that for almost the complete examined range, the observed q_a values are systematically higher than the corresponding curve from random data.

It is interesting to comment the very different behavior of the false identification of accelerated and decelerated deformation patterns when applied to random catalogues. This different behavior could be a result either of the different constraints used for the two patterns or of the manner that the random catalogues are created, as only aftershock sequences are taken into account in their generation besides the "standard" mainshock seismicity. It is possible that other patterns which are observed in nature due to the stress loading–unloading processes may result in more complicated space–time seismicity patterns, which are not reflected in the random catalogues used in the present work. On the other hand, the results obtained from random catalogues clearly demonstrate that the combined use of both the accelerated and decelerated deformation behavior can significantly reduce the possibility of false alarms when attempting to predict future events, at least due to the catalogue randomness.

7. Implications for earthquake prediction

The results of the present work, which are based on mainshocks that have already occurred in five different seismotectonic regimes, provide the base for the suggestion of a "Decelerating In–Accelerating Out Strain" model which can be used towards the prediction of future mainshocks and estimate relative uncertainties. A possible approach for this estimation can be performed by applying the complete procedure which has been previously described for the identification of regions of accelerating and decelerating strain; however, calculations should be repeated for several assumed values of the origin time and magnitude of the mainshock. As centers of such regions which correspond to best solutions, we have considered the grid points for which the quality index, q, takes its largest value because q (relations (6) and (10)) quantifies not only the increase of deviation from linearity (small C) but also the degree of compatibility with properties of already occurred preshock sequences (large P). Once the two regions and their parameters are determined, the estimation of the mainshock parameters (origin time, magnitude, epicenter) is described in detail in the following.

For the estimation of the predicted origin time, t_c*, of the probably ensuing mainshock, the average of the two values calculated by relations (5) and (9) is considered. Furthermore, the value of the mainshock magnitude corresponding to the best solution for the accelerating strain (relations (3) and (4)) and the corresponding value to the best solution for the decelerating strain (relation

(8)) can be used to obtain an average value for the predicted magnitude, M^*, of the probably ensuing mainshock.

For the determination of the epicenter of the expected mainshock, we have considered four points which are determined before the generation of a mainshock and their locations are related to the location of the oncoming mainshock. These points are (a) the geometrical center, F, of the region of the decelerating strain, (b) the center, P_f, of the epicenters of the decelerating preshocks which can be considered as the physical center of the region of decelerating strain, (c) the geometrical center, Q, of the region of accelerating strain, and (d) the center, P_q, of the epicenters of the accelerating preshocks which can be considered as the physical center of the region of accelerating strain. We have performed a large number of tests regarding the way by which these four points can be used to locate the expected mainshock epicenter. These tests showed that the best estimation is obtained when using the middle point, D, of the line segment FP_f and the middle point, A, of the line segment QP_q and considering their distances DE and AE from the mainshock epicenter. From the 46 preshock–mainshock sequences investigated in the present work, it was found that $DE=100\pm40$ km and $AE=180\pm80$ km, where 40 and 80 km are the corresponding standard deviations. Based on these results, the epicenter of the ensuing mainshock can be estimated by the following procedure: in those cases when the two circles (D, 100 km; A, 180 km) overlap, a unique solution cannot be defined and D (defined from the decelerating pattern) can be considered as the predicted mainshock epicenter, $E*$. In the other cases, when the two circles do not intersect, the point of the circle (D, 100 km) which is closer to the circle (A, 180 km) is considered as the predicted mainshock epicenter.

In order to estimate the prediction uncertainty, the previous approach has been applied to retrospectively (a posteriori) predict the parameters (origin time, magnitude, epicenter coordinates) of each one of the 46 mainshocks considered in the present work. The epicenter coordinates, $E^*(\varphi,\lambda)$, origin times, t_c^*, and magnitudes, M^*, predicted by this method are listed in Table 1. The mean distance between the predicted, E^*, and the observed, E, epicenter and the corresponding standard deviation is $E^*E=80\pm35$ km. Hence, considering the two standard deviation model uncertainty ($2\sigma=70$ km) indicates that the epicenter location can be predicted with an error less than 150 km with high probability (~0.95), without considering random catalogue artifacts. The corresponding mean difference between predicted, t_c^*, and observed, t_c, origin time is almost zero with a standard deviation equal to 1.2 years, which suggests that the origin time can be predicted with an error ±2.5 years with similar probability. Finally, the average difference between the predicted, M^*, and the observed, M, magnitude is also almost zero and the standard deviation is 0.2; hence, the mainshock magnitude estimation exhibits a typical error ±0.4 with a similar probability.

We should point out that the application of the proposed model was almost impossible for Northern Japan for events of the order of $M\sim6.0$–7.0, as also previously mentioned. Despite the apparent failure of the model, this result is in good agreement with Eqs. (5) and (9) which predict very small durations of the preshock period, due to the very high seismicity rate of the area (very large s_a and s_d values), which lead to a space–time overlap of such events. The corresponding patterns are more evident for larger events ($M\geq7.0$) due to the much larger areas affected and "controlled" by such events, as is also correctly predicted by relations (3) and (8), where the preparation area size scales with the expected mainshock magnitude.

8. Discussion

Decelerating strain in the narrower seismogenic region and accelerating strain in the broader critical region at about the same time period has been observed in all 46 cases, which concern five complete samples of recent (since 1980) mainshocks occurred in five different seismotectonic regimes (W. Mediterranean, Aegean, Anatolia, California, Japan). These observations indicate that the proposed "Decelerating In–Accelerating Out Strain" pattern is probably of general validity. This conclusion is further supported by the fact that several investigators have independently observed similar precursory accelerating generation of intermediate-magnitude shocks (preshocks) for many strong mainshocks, while other researchers observed precursory intermediate-term seismic quiescence (decrease of the number of small shocks) in the narrower fault zone for a large number of mainshocks.

In the present work, the time variation of Benioff strain of both preshock sequences (accelerating and decelerating) is studied by taking into consideration information on both the time variation of the frequency and of the magnitude of preshocks, since Benioff strain is affected by both these quantities. The method relies on the use of intermediate-magnitude preshocks ($M_{min}\geq4.0$, see Tables 2 and 3) for which completeness is easily attained nowadays. The time variation of Benioff strain is well fitted by a power-law (relation (1)) not only for

accelerating preshock sequences (average $\bar{C}=0.44\pm0.09$) but also for decelerating preshock sequences (average $\bar{C}=0.35\pm0.09$). On the other hand, by considering seismic strain in the seismogenic region as decelerating, which requires a seismic excitation at the start phase of each decelerating sequence, we implicitly take also into consideration such seismic excitation which is considered by some investigators as an important predictive precursor (Evison and Rhoades, 1977; Evison, 2001).

The results suggest that the model uncertainties are of the order of ±0.4 for the mainshock magnitude, ±2.5 years for the origin time and less than 150 km for the epicenter, with high confidence (~95%). Furthermore, the combination of accelerating and decelerating deformation patterns ensures a rather small probability of artificial observation of the previous patterns, as tests on synthetic catalogues for one of the studied areas have shown a small probability of random combined occurrence (~10% or less). However, it must be emphasized that these uncertainties are only indicative of the robustness of the model. The practical predictive capacity of the method (percentage of false alarms, etc.) and its real uncertainties can be reliably defined only by a forward procedure, that is, by attempting predictions of future strong earthquakes, a direction on which we are currently working.

Acknowledgments

Some of the maps have been produced with the GMT software (Wessel and Smith, 1995). This work has been partly financed by the project “Pythagoras” funded by the EPEAEK under Project 21891 and partly by the Earthquake Protection and Planning Organization of Greece (Project 20242) of the Aristotle University of Thessaloniki Research Committee.

References

Allègre, C.J., Le Mouël, J.L., 1994. Introduction of scaling techniques in brittle failure of rocks. Phys. Earth Planet. Inter. 87, 85–93.

Ben-Zion, Y., Lyakhovsky, 2002. Accelerated seismic release and related aspects of seismicity patterns on earthquake faults. Pure Appl. Geophys. 159, 2385–2412.

Ben-Zion, Y., Dahmen, K., Lyakhovsky, V., Ertas, D., Agnon, A., 1999. Self-driven mode switching of earthquake activity on a fault system. Earth Planet. Sci. Lett. 172, 11–21.

Bowman, D.D., Quillon, G., Sammis, C.G., Sornette, A., Sornette, D., 1998. An observational test of the critical earthquake concept. J. Geophys. Res. 103, 24359–24372.

Bufe, C.G., Varnes, D.J., 1993. Predictive modeling of seismic cycle of the Great San Francisco Bay Region. J. Geophys. Res. 98, 9871–9883.

Bufe, C.D., Nishenko, S.P., Varnes, D.J., 1994. Seismicity trends and potential for large earthquakes in Alaska–Aleutian region. Pure Appl. Geophys. 142, 83–99.

Chouliaras, G., Stavrakakis, G., 2001. Current seismic quiescence in Greece: implications for seismic hazard. J. Seismol. 5, 595–608.

Dobrovolsky, J.P., Zubkov, S.I., Miachkin, B.J., 1979. Estimation of the size of earthquake preparation zones. Pure Appl. Geophys. 117, 1025–1044.

Evison, F.F., 2001. Long-range synoptic earthquake forecasting: an aim for the millennium. Tectonophysics 333, 207–215.

Evison, F.F., Rhoades, 1977. The precursory earthquake swarm in New Zealand. N.Z. J. Geol. Geophys. 40, 537–547.

Guarino, A.S., Ciliberto, S., Garcimartin, A., 1999. Failure time and microcrack nucleation. Europhys. Lett. 47, 456–461.

Hainzl, S., Zöller, G., Kurths, J., Zschau, J., 2000. Seismic quiescence as an indicator for large earthquakes in a system of self-organized criticality. Geophys. Res. Lett. 27, 597–600.

Jaumè, S.C., 1992. Moment release rate variations during the seismic circle in the Alaska–Aleutians subduction zone, extended abstract. Proceed. Wadati Conference on Great Subduction Earthquakes. University of Alaska, pp. 123–128.

Kanamori, H., 1981. The nature of seismicity patterns before large earthquakes. In: Ewing, M., Simpson, D., Richards, P. (Eds.), Earthquake Prediction, an International Review, Series 4. Am. Geophys. Union, Washington, pp. 1–19.

Karakaisis, G.F., Scordilis, E.M., Papazachos, C.B., Papazachos, B. C., 2005. A catalogue of earthquakes in California for the period 1901–2004. Publ. Geoph. Laboratory. University of Thessaloniki.

Kato, N., Ohtake, M., Hirasawa, T., 1997. Possible mechanism of precursory seismic quiescence: regional stress relaxation due to preseismic sliding. Pure Appl. Geophys. 150, 249–267.

Knopoff, L., Levshina, T., Keilis-Borok, V.J., Mattoni, C., 1996. Increase long-range intermediate-magnitude earthquake activity prior to strong earthquakes in California. J. Geophys. Res. 101, 5779–5796.

Mogi, K., 1962. On the time distribution of aftershocks accompanying the recent major earthquakes in and near Japan. Bull. Earthq. Res. Inst. Univ. Tokyo 40, 107–124.

Mogi, K., 1969. Some features of the recent seismic activity in and near Japan II. Activity before and after great earthquakes. Bull. Earthq. Res. Inst. Univ. Tokyo 47, 395–417.

Papadopoulos, G.A., 1986. Long term earthquake prediction in western Hellenic arc. Earthq. Predict. Res. 4, 131–137.

Papaioannou, Ch., Papazachos, B.C, 2000. Time-independent and time-dependent seismic hazard in Greece based on seismogenic sources. Bull. Seismol. Soc. Am. 90, 22–33.

Papazachos, B.C., 1974a. On certain foreshock and aftershock parameters in the area of Greece. Ann. Geofis. 27, 497–515.

Papazachos, B.C., 1974b. On the time distribution of aftershocks and foreshocks in the area of Greece. Pure Appl. Geophys. 112, 627–631.

Papazachos, C.B., 2001. An algorithm of intermediate-term earthquake prediction using a model of accelerating seismic deformation. 2nd Hellenic Conference on Earthquake Engineering and Engineering Seismology, 28–30 November 2001, pp. 107–115.

Papazachos, C.B., 2003. Minimum preshock magnitude in critical regions of accelerating seismic crustal deformation. Boll. Geofis. Teor. Appl. 44, 103–113.

Papazachos, B.C., Papazachou, C.B., 1997. Earthquakes of Greece. Ziti Publ, Thessaloniki. 304 pp.

Papazachos, B.C., Papazachos, C.B., 2000. Accelerated preshock deformation of broad regions in the Aegean area. Pure Appl. Geophys. 157, 1663–1681.

Papazachos, C.B., Papazachos, B.C., 2001. Precursory accelerating Benioff strain in the Aegean area. Ann. Geofis. 144, 461–474.

Papazachos, C.B., Karakaisis, G.F., Savvaidis, A.S., Papazachos, B.C., 2002. Accelerating seismic crustal deformation in the southern Aegean area. Bull. Seismol. Soc. Am. 92, 570–580.

Papazachos, C.B., Karakaisis, G.F., Scordilis, E.M., Papazachos, B.C., 2004a. Probabilities of activation of seismic faults in critical regions of the Aegean area. Geophys. J. Int. 159, 679–687.

Papazachos, C.B., Scordilis, E.M., Karakaisis, G.F., Papazachos, B.C., 2004b. Decelerating preshock seismic deformation in fault regions during critical periods. Bull. Geol. Soc. Greece 36, 1–9.

Papazachos, C.B., Karakaisis, G.F., Scordilis, E.M., Papazachos, B.C., 2005a. Global observational properties of the critical earthquake model. Bull. Seismol. Soc. Am. 95, 1841–1855, doi:10.1785/120040181.

Papazachos, B.C., Comninakis, P.E., Scordilis, E.M., Karakaisis, G.F., Papazachos, C.B., 2005b. A catalogue of earthquakes in the Mediterranean and surrounding area for the period 1901–2004. Publ. Geoph. Laboratory. University of Thessaloniki.

Raleigh, C.B., Sieh, K., Sykes, L.R., Anderson, D.L., 1982. Forecasting Southern California earthquakes. Science 217, 1097–1104.

Rundle, J.B., Klein, W., Turcotte, D.L., Malamud, B.D., 2000. Precursory seismic activation and critical point phenomena. Pure Appl. Geophys. 157, 2165–2182.

Rundle, J.B., Turcotte, D.L., Shcherbakov, R., Klein, W., Sammis, C., 2003. Statistical physics approach to understanding the multi-scale dynamics of earthquake fault systems. Rev. Geophys. 41, 5/1–5/30.

Scholz, Ch.H., 1988. Mechanism of seismic quiescences. Pure Appl. Geophys. 26, 701–718.

Scordilis, E.M., 2006. Empirical global relations converting MS and mb to moment magnitude. J. Seismol. doi:10.1007/s10950-006-9013-3.

Scordilis, E.M., Karakaisis, G.F., Papazachos, C.B., Papazachos, B.C., 2005. A Catalogue of Earthquakes in Japan for the Period 1901–2004. Publ. Geoph. Laboratory. University of Thessaloniki.

Sornette, D., Sammis, C.G., 1995. Complex critical exponents from renormalization group theory of earthquakes: implications for earthquake predictions. J. Phys., I 5, 607–619.

Sornette, A., Sornette, D., 1990. Earthquake rupture as a critical point. Consequences for telluric precursors. Tectonophysics 179, 327–334.

Sykes, L.R., Jaumè, S., 1990. Seismic activity on neighboring faults as a long term precursor to large earthquakes in the San Francisco Bay area. Nature 348, 595–599.

Tocher, D., 1959. Seismic history of the San Francisco bay region. Calif. Div. Mines Spec. Rep., vol. 57, pp. 39–48.

Tzanis, A., Vallianatos, F., 2003. Distributed power law seismicity changes and crustal deformation in the SW Hellenic Arc. Nat. Hazards Earth Sys. Sci. 3, 179–195.

Tzanis, A., Vallianatos, F., Makropoulos, K., 2000. Seismic and electrical precursors to the 17-1-1983, $M=7$ Kefallinia earthquake, Greece, signatures of a SOC system. Phys. Chem. Earth, A 25, 281–287.

Wessel, P., Smith, W., 1995. New version of the generic mapping tools. EOS 76–329.

Wyss, M., Habermann, R.E., 1988. Precursory seismic quiescence. Pure Appl. Geophys. 126, 319–332.

Wyss, M., Klein, F., Johnston, A.C., 1981. Precursors of the Kalapana $M=7.2$ earthquake. J. Geophys. Res. 86, 3881–3900.

Zöller, G., Hainzl, S., 2002. A systematic spatiotemporal test of the critical point hypothesis for large earthquakes. Geophys. Res. Lett. 29, 1558–1561.

Zöller, G., Hainzl, S., Kurths, J., 2001. Observation of growing correlation length as an indicator for critical point behavior prior to large earthquakes. J. Geophys. Res. 106, 2167–2175.

Zöller, G., Hainzl, S., Kurths, J., Zschau, J., 2002. A systematic test on precursory seismic quiescence in Armenia. Nat. Hazards 26, 245–263.